Classical Stark Mixing at Ultralow Collision Energies

D. Vrinceanu and M. R. Flannery
School of Physics, Georgia Institute of Technology, Atlanta, Georgia 30332
(Received 15 May 2000)

Exact solutions of the time-dependent classical equations are obtained for the full array of angular momentum mixing transitions $n\ell \rightarrow n\ell'$ in atomic hydrogen induced by collisions with charged particles at ultralow energies. A novel classical expression for the transition probability $P_{\ell'\ell}$ is presented. The exact classical results for $P_{\ell'\ell}(\alpha)$ as a function of ℓ, ℓ' and the Stark parameter α agree exceptionally well with (exact) quantal results. They complement the quantal results by revealing essential characteristics which remain obscured in the quantal treatment.

PACS numbers: 34.50.Pi, 34.10.+x, 34.60.+z

Stark mixing occurs when the electron of a Rydberg atom (in a state with principal quantum number n) changes its angular momentum, without changing its energy, as a result of a collision, at large impact parameter b, with a slow massive particle of charge $Z_1 e$ moving with velocity v. It is a subject of broad interest and importance in many areas of modern physics [1] and chemistry [2], astrophysics [3], line broadening [4], Auger processes [5], and for antihydrogen formation by three-body recombination [6,7] at ultracold temperatures. Although remarkable effort has been devoted to obtaining theoretical solutions for Stark mixing in Rydberg atoms to various levels of approximation [1–13], the purpose of this Letter is to point out that the problem is capable of an exact solution in the classical formulation. The exceptionally rich dynamical SO(4) symmetry of $H(n, \ell)$ is the key foundation which allows both classical and quantal exact solutions to be constructed [14] in a similar and unified way. There is substantial renewed [1,15–19] interest in the power of classical dynamics in almost all fields of modern physics, attributed to the desire [15,19] to obtain a more thorough understanding of the classical-quantal correspondence. Stark mixing by ion impact is probably the last problem in collision physics which is capable of an exact solution.

The present new treatment is not an extension of any previous theory and is capable of providing the first comprehensive classical solution for the full array $n\ell \rightarrow n\ell'$ of collisional transitions in $H(n, \ell)$. A new expression for the classical transition probability $P_{\ell'\ell}$ is defined in a language which exploits the dynamical symmetry. The derived probability for the general array $\ell \rightarrow \ell'$ of transitions has a very simple functional form, can be easily calculated for any principal quantum number, and provides physical insight and simple geometrical explanations for the behavior of the transition probabilities. Stark mixing probabilities are calculated and compared with the (exact) quantal results [14,20]. Considering the Rydberg atom in a frame which rotates together with the internuclear axis, the Stark mixing problem can in principle be reduced [11,12] to the problem of the Rydberg atom in mixed *static* electric and magnetic fields. This approach is successful only for the particular case of $\ell = 0$, which is fully recovered by the present general fixed frame formulation.

The target Rydberg atom (with averaged electron orbit radius a_n, velocity v_n, momentum p_n, and angular frequency $\omega_n = v_n/a_n$) is centered at the origin O of a fixed coordinate frame. The trajectory of the projectile, initially moving with impact parameter b along the positive Z direction, is assumed to be confined in the YOZ plane. In addition to the energy E, constant along the Hamiltonian $H_0 = p^2/2m_e - e^2/r$, the angular momentum $\mathbf{L} = \mathbf{r} \times \mathbf{p}$ of the unperturbed Rydberg electron and the Runge-Lenz (or eccentricity) vector,

$$\mathbf{A} = p_n^{-1}\left[\mathbf{p} \times \mathbf{L} - m_e e^2 \frac{\mathbf{r}}{r}\right], \tag{1}$$

directed toward the pericenter and normalized to angular momentum units, are also conserved. These quantities define the dynamic SO(4) symmetry of the hydrogen atom. Because the SO(4) group is isomorphic with the direct product SO(3) $\oplus$ SO(3) of two rotation groups, a special decomposition, $\mathbf{L} = \mathbf{M} + \mathbf{N}$ and $\mathbf{A} = \mathbf{M} - \mathbf{N}$, permits the dynamics of the hydrogen atom to be separated into two decoupled motions. The generators $\mathbf{M}$ and $\mathbf{N}$ act independently as angular momenta and are also conserved quantities for the unperturbed Rydberg atom. They evolve independently [21] with time on application of a constant electric field $\vec{\mathcal{E}}$ and precess about $\vec{\mathcal{E}}$ with the Stark frequencies $\vec{\omega}_S = \mp(3/2)a_n v_n(\vec{\mathcal{E}}/e)$. For weak fields, the Stark splitting $\Delta E_S = \hbar\omega_S < \hbar\omega_n = \Delta E_n$, the $(n \rightarrow n \pm 1)$ energy splitting. For constant fields, the vectors $\mathbf{L}$ and $\mathbf{A}$ vary periodically with frequency ω_S.

The weak field approximation assumes that the time-dependent electric field $\vec{\mathcal{E}}(t)$ generated by the passing projectile of charge $Z_1 e$ is constant over the atom's spatial extent and the dipole approximation for interaction potential $V = e\vec{r} \cdot \vec{\mathcal{E}}$ is valid. Hence

$$\vec{\mathcal{E}}(t) = -\frac{Z_1 e \hat{R}}{R^2} = \frac{Z_1 e}{v b}\frac{d\Phi}{dt}\hat{R},$$

where Φ is the polar angle between the internuclear vector $\mathbf{R}$ and the Z axis.

 0031-9007/00/85(23)/4880(4)$15.00

On assuming that the collision is orbital adiabatic ($\dot{\Phi} < \omega_n$), $\vec{\mathcal{E}}$ is constant over one period so that the slow rate of variation $\Delta\mathbf{L}/T$ of the angular momentum over one orbital period $T = 2\pi/\omega_n$, is the classical average

$$\frac{d\mathbf{L}}{dt} = -\frac{e}{T}\int_0^T (\mathbf{r} \times \vec{\mathcal{E}})\, dt = -e\langle \mathbf{r}\rangle \times \vec{\mathcal{E}}(t)\,.$$

Since the weak field approximation ($\omega_S < \omega_n$) also holds, the vectors $\mathbf{L}$ and $\mathbf{A}$ change very little over one orbital period and $\langle \mathbf{r}\rangle \approx -3\mathbf{A}/2p_n = -3\ \mathbf{A}(a_n v_n/2e^2)$. The following set [3],

$$\frac{d\mathbf{L}}{dt} = -\omega_S \hat{R} \times \mathbf{A}, \qquad \frac{d\mathbf{A}}{dt} = -\omega_S \hat{R} \times \mathbf{L}\,,$$

of coupled equations can then be deduced, where both $\hat{R}$ and $\omega_S = \alpha\dot{\Phi}$ now vary with time. The Stark parameter α is $3Z_1 a_n v_n/2bv$. The weak field ($\omega_S < \omega_n$) and adiabatic ($\dot{\Phi} < v_n/a_n$) conditions combine to yield the partitioning $b \geq (v/v_n)a_n$, when $v \geq v^* = (3Z_1/2)^{1/2}v_n$, and $b \geq (3Z_1/2)^{1/2}a_n$, when $v \leq v^*$, of (v, b) space for validity of the present solutions. For $v \geq v^*$, α remains ≤ 1. For $v < v^*$, α can exceed unity. When written in terms of vectors $\mathbf{M}$ and $\mathbf{N}$, the above set of differential equations yields the set of decoupled equations,

$$\frac{d\mathbf{M}}{d\Phi} = -\alpha \hat{R} \times \mathbf{M}, \qquad \frac{d\mathbf{N}}{d\Phi} = +\alpha \hat{R} \times \mathbf{N}\,. \tag{2}$$

Since the magnitudes $M^2 = N^2 = (L^2 + A^2)/4 = n^2\hbar^2/4$ remain constant throughout the collision, exact solutions of Eqs. (2) can then be obtained [14] at general angle Φ in terms of finite rotations from the initial values $\mathbf{M}(\Phi_0)$ and $\mathbf{N}(\Phi_0)$, via the orthogonal transformations $\mathbf{M}(\Phi) = U_M(\Phi, \Phi_0)\mathbf{M}(\Phi_0)$ and $\mathbf{N}(\Phi) = U_N(\Phi, \Phi_0)\mathbf{N}(\Phi_0)$. For example, if the initial state is specified by the vectors $(\mathbf{L}, \mathbf{A})$ at $\Phi_0 = \pi$, then the final state $(\mathbf{L}', \mathbf{A}')$, at $\Phi = 0$, is determined by the rule

$$\begin{aligned}
L_1' &= \gamma^{-2}[1 + \alpha^2\cos(\pi\gamma)]L_1 + \alpha\gamma^{-1}\sin(\pi\gamma)A_2 + \alpha\gamma^{-2}[1 - \cos(\pi\gamma)]A_3\,,\\
L_2' &= -\cos(\pi\gamma)L_2 - \gamma^{-1}\sin(\pi\gamma)L_3 + \alpha\gamma^{-1}\sin(\pi\gamma)A_1\,,\\
L_3' &= \gamma^{-1}\sin(\pi\gamma)L_2 - \gamma^{-2}[\alpha^2 + \cos(\pi\gamma)]L_3 + \alpha\gamma^{-2}[\cos(\pi\gamma) - 1]A_1\,,\\
A_1' &= \gamma^{-2}[1 + \alpha^2\cos(\pi\gamma)]A_1 + \alpha\gamma^{-1}\sin(\pi\gamma)L_2 + \alpha\gamma^{-2}[1 - \cos(\pi\gamma)]L_3\,,\\
A_2' &= -\cos(\pi\gamma)A_2 - \gamma^{-1}\sin(\pi\gamma)A_3 + \alpha\gamma^{-1}\sin(\pi\gamma)L_1\,,\\
A_3' &= \gamma^{-1}\sin(\pi\gamma)A_2 - \gamma^{-2}[\alpha^2 + \cos(\pi\gamma)]A_3 + \alpha\gamma^{-2}[\cos(\pi\gamma) - 1]L_1\,.
\end{aligned} \tag{3}$$

Here $\gamma = \sqrt{1 + \alpha^2}$ and the components of the initial and final vectors are defined in the fixed coordinate frame considered. The above exact solutions (3) are easily verified and satisfy the invariant relations

$$\mathbf{L}' \cdot \mathbf{A}' = \mathbf{L} \cdot \mathbf{A} = 0 \tag{4}$$

and

$$\mathbf{L}'^2 + \mathbf{A}'^2 = \mathbf{L}^2 + \mathbf{A}^2 = n^2\hbar^2. \tag{5}$$

The orbit of the final state $(n, \mathbf{L}')$ is confined to a plane perpendicular to the final $\mathbf{L}'$ and the energy is preserved (since n does not change). The above constraints, Eqs. (4) and (5), define in the $(\mathbf{L}, \mathbf{A})$ space a hypersurface on which the initial state, defined by the initial angular momentum quantum number ℓ, is uniformly distributed. The volume of this hypersurface is therefore given by

$$\mathcal{V}_{n\ell} = \iint \delta(|\mathbf{L}| - \hbar\ell)\delta(|\mathbf{A}| - \hbar\sqrt{n^2 - \ell^2})\delta(\mathbf{L} \cdot \mathbf{A})\, d\mathbf{L}\, d\mathbf{A}\,. \tag{6}$$

Each point from this manifold evolves during the collision according to the rule (3), so that only a fraction of possible initial states can produce the final state with angular momentum quantum number ℓ', after the collision. The volume of $(\mathbf{L}, \mathbf{A})$ space which overlaps the initial and final states is

$$\mathcal{V}_{n\ell\ell'} = \iint \delta(|\mathbf{L}| - \ell\hbar)\delta(|\mathbf{L}'| - \ell'\hbar)\delta(|\mathbf{A}| - \hbar\sqrt{n^2 - \ell^2})\delta(\mathbf{L} \cdot \mathbf{A})\, d\mathbf{L}\, d\mathbf{A}\,. \tag{7}$$

The $\ell \to \ell'$ transition probability is then, in a geometric sense, the ratio of the two volumes

$$P_{\ell'\ell}^{(n)} = \frac{\mathcal{V}_{n\ell\ell'}}{\mathcal{V}_{n\ell}}\,. \tag{8}$$

This is a novel result in that Eq. (8) is defined in terms of the new $(\mathbf{L}, \mathbf{A})$ representative space, being more appropriate, than the customary $(\mathbf{r}, \mathbf{p})$ phase space, for direct expression of the dynamical SO(4) symmetry of $H(n, \ell)$.

The six-dimensional integral (6) can be calculated directly, while the integral (7) eventually reduces to yield the one-dimensional integral [14]

$$P_{\ell'\ell}^{(n)} = \frac{2\ell'}{\pi\hbar n^2}\,\frac{1}{1 - \cos\chi}\int \frac{dz}{\sqrt{(z^2 - \mathcal{A})(\mathcal{B} - z^2)}}$$

for the transition probability. This, in turn, may be expressed in terms of the complete elliptic integral,

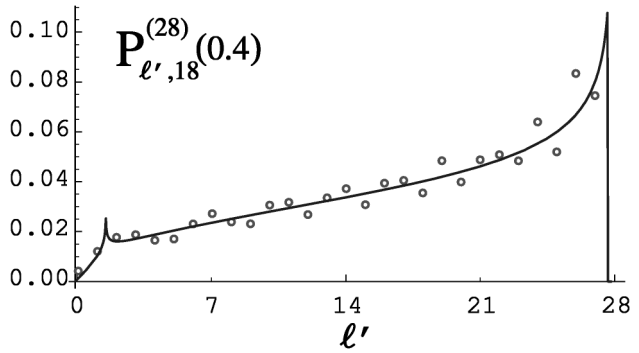

FIG. 1. Probability for the $18 \to \ell'$ transition, within the $n = 28$ energy shell, for a given Stark parameter $\alpha = 0.4$. Exact quantal results are denoted by dots.

$K(m) = \int_0^{\pi/2}(1 - m\sin^2 x)^{-1/2}\,dx$, as

$$P^{(n)}_{\ell'\ell}(\chi) = \frac{2\ell'/n^2}{\pi\hbar\sin^2(\chi/2)}\begin{cases} 0, & \mathcal{B} < 0, \\ \frac{K[\mathcal{B}/(\mathcal{B}-\mathcal{A})]}{\sqrt{\mathcal{B}-\mathcal{A}}}, & \mathcal{B} > 0, \mathcal{A} < 0, \\ \frac{K[(\mathcal{B}-\mathcal{A})/\mathcal{B}]}{\sqrt{\mathcal{B}}}, & \mathcal{B} > 0, \mathcal{A} > 0, \end{cases} \tag{9}$$

where

$$\mathcal{A}(\ell/n, \ell'/n; \chi) = \frac{\cos(u_1 + u_2) - \cos\chi}{1 - \cos\chi}, \qquad \mathcal{B}(\ell/n, \ell'/n; \chi) = \frac{\cos(u_1 - u_2) - \cos\chi}{1 - \cos\chi}. \tag{10}$$

The angles u_1 and u_2 depend only on the initial and final states via $\cos u_1 = 2\ell^2/n^2 - 1$ and $\cos u_2 = 2\ell'^2/n^2 - 1$. The rotation angle χ, which depends only on the Stark parameter α and the polar angle $\Delta\Phi = \Phi - \Phi_0$ swept out during the collision time interval (t_0, t), is determined by

$$\cos\frac{\chi}{2} = [1 + \alpha^2\cos(\sqrt{1+\alpha^2}\,\Delta\Phi)]/(1+\alpha^2).$$

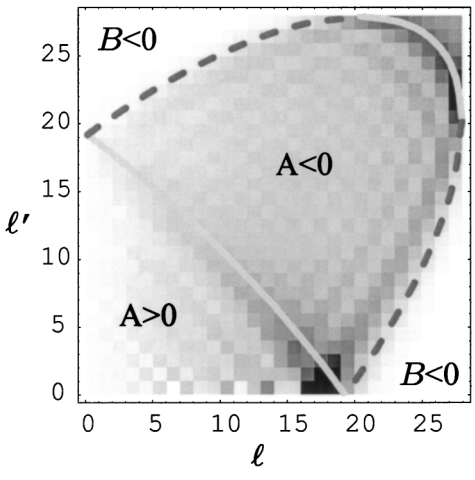

FIG. 2. Density plots of the $\ell \to \ell'$ transition probabilities, calculated within the quantal treatment for $\alpha = 0.4$ and $n = 28$. The probabilities increase as the color becomes darker. The continuous and broken lines represent the classical $\mathcal{A} = 0$ and $\mathcal{B} = 0$ ridges.

The condition $\mathcal{B} < 0$ defines the classical inaccessible region. Two types of singular points are apparent from the solution (9). At $\mathcal{B} = 0$, the transition probability $P_{\ell'\ell}(\alpha)$ has a finite jump (step discontinuity) and at $\mathcal{A} = 0$ it has a logarithmic (cusp) singularity. These features are displayed in Figs. 1–5 for representative transitions. For a given Stark parameter α and initial angular momentum ℓ, the solutions of the equations $\mathcal{A} = 0$ and $\mathcal{B} = 0$ provide the critical values

$$\ell'_{\pm} = \ell\left|\cos\frac{\chi}{2} \pm \left(\frac{n^2}{\ell^2} - 1\right)^{1/2}\sin\frac{\chi}{2}\right|$$

of the final angular momentum, where the cusp or step singularities are located. The inequality $\mathcal{A} < \mathcal{B}$ is strictly fulfilled except for the limiting cases of ℓ or $\ell' \to 0$ or n when $\mathcal{A} = \mathcal{B}$. These limits are readily deduced from Eq. (9) to provide the following probabilities:

$$P^{(n)}_{\ell'0}(\alpha) = \frac{\ell'/(\hbar n^2)}{\sin(\chi/2)\sqrt{\sin^2(\chi/2) - (\ell'/n)^2}},$$

$$P^{(n)}_{\ell' n}(\alpha) = \frac{\ell'/(\hbar n^2)}{\sin(\chi/2)\sqrt{(\ell'/n)^2 - \sin^2(\chi/2)}},$$

$$P^{(n)}_{n\ell}(\alpha) = \frac{1/(\hbar n)}{\sin(\chi/2)\sqrt{(\ell/n)^2 - \sin^2(\chi/2)}}.$$

The $\ell \to \ell' = 0$ transitions have zero classical probability. The specific case [12] of $0 \to \ell'$ transitions is therefore directly recovered from our general result (9).

Figure 1 shows the classical probability $P^{(28)}_{\ell',18}$ for the representative array $\ell = 18 \to \ell'$ transitions. The quantal results [14,20] oscillate about the classical background. Figure 1 also displays the $\mathcal{A} = 0$ cusp at ℓ'_- followed by the $\mathcal{B} = 0$ downward step at ℓ'_+, as ℓ' is increased from 0 to n. In the central region $\mathcal{A} < 0$ and $\mathcal{B} > 0$.

Figure 2 provides the density map of the quantal probabilities [14,20] for the full array of $\ell \to \ell'$ transitions at $\alpha = 0.4$. In the classical forbidden regions (where $\mathcal{B} < 0$), the upper left and lower right corners, the quantal probabilities decrease exponentially. The lines of singularities $\mathcal{A} = 0$ and $\mathcal{B} = 0$ are also shown. Along these,

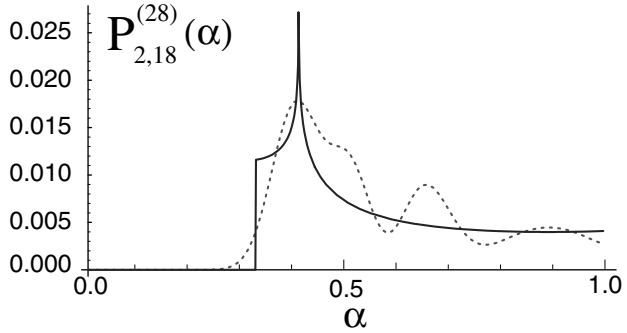

FIG. 3. Probability for the $18 \to 2$ transition, within the $n = 28$ energy shell, as a function of the Stark parameter α. Exact quantal results: dotted line.

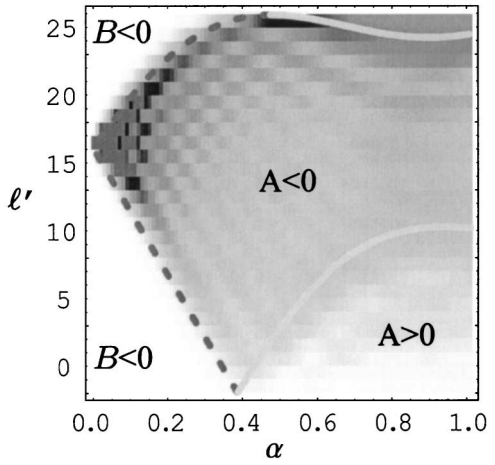

FIG. 4. Density plots of the $\ell = 18 \rightarrow \ell'$ transition probabilities, calculated within the quantal treatment for $n = 28$, as a function of α.

the classical transition probabilities display cusp and step-like behavior, respectively, and, in their vicinity, the quantal results have local maxima. Figure 1 follows from a vertical line drawn through the plot at $\ell = 18$, showing a cusp-step variation. Figure 2 predicts step-step and step-cusp variations for transitions from $\ell > 19$.

In Fig. 3, the classical and quantal transition probabilities for the $18 \rightarrow 2$ transition are plotted as a function of the Stark parameter α. This plot can also be obtained by following the variation of the transition probability along a horizontal line with $\ell' = 2$ in Fig. 4.

Figure 4 presents a density map for the quantal probabilities for transition from the initial angular momentum $\ell = 18$ to any ℓ' and for any value of α. As $\alpha \rightarrow 0$ the span of possible final angular momenta is reduced, such that only elastic transitions are possible at $\alpha = 0$. The classical singularity lines $\mathcal{A} = 0$ and $\mathcal{B} = 0$ illustrate again the correspondence with the quantal results. The cusp-step pattern of Fig. 1 is also explained by a vertical line at $\alpha = 0.4$ of Fig. 4. For low $\alpha < 0.4$, a step-step variation is predicted, i.e., the accessible ℓ' lie within the range $\ell'_- < \ell' < \ell'_+$. The results in Fig. 5 confirm this prediction. Cusp-cusp patterns occur at higher $\alpha \geq 0.5$.

In conclusion, the exact solution (3) of the classical equations (2) has been obtained, by exploiting the SO(4) dynamical symmetry of $H(n, \ell)$. The novel expression (8) provides the general result (9) for the classical probability $P^{(n)}_{\ell\ell'}$ for the full array of Stark mixing transitions $n\ell \rightarrow n\ell'$. Since $\mathcal{A}$ and $\mathcal{B}$ are symmetrical in (ℓ, ℓ') the probability (9) satisfies the detailed balance relation $2\ell P^{(n)}_{\ell'\ell} = 2\ell' P^{(n)}_{\ell\ell'}$. Probability conservation $\int_0^n P^{(n)}_{\ell'\ell} \hbar d\ell' = 1$ is also satisfied. Cross sections [14] may be calculated from Eq. (9). Exceptional agreement is obtained between the classical and quantal $P^{(n)}_{\ell\ell'}(\alpha)$ as a function of ℓ, ℓ' and the Stark parameter α. The common SO(4) symmetry provides this classical-quantal correspondence at a level more fundamental than Ehrenfest's theorem and the Heisenberg correspondence. The classical method is also complementary in that it reveals very succintly essential and valuable characteristics which remain obscured within the quantal treatment. This reflects the essential power of classical dynamics when applied to collision problems.

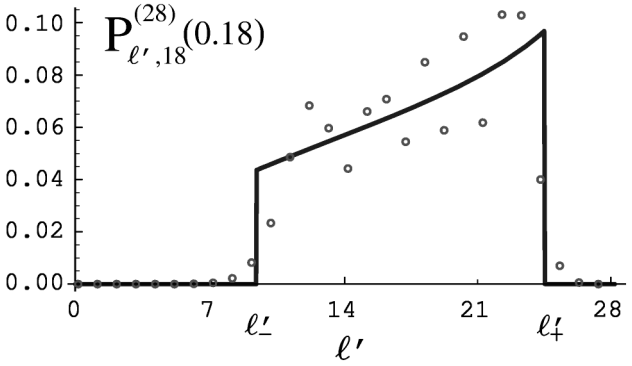

FIG. 5. As in Fig. 1, but for Stark parameter $\alpha = 0.18$.

This work has been supported by AFOSR Grant No. 49620-99-1-0277 and NSF Grant No. 98-02622.

[1] V. S. Lebedev and I. L. Beigman, *Physics of Highly Exited Atoms and Ions* (Springer-Verlag, Berlin, 1998).
[2] F. Merkt and R. N. Zare, J. Chem. Phys. **101**, 3495 (1994).
[3] I. Percival, *Atoms in Astrophysics* (Plenum, New York, 1983), pp. 75–102.
[4] D. Hoang-Binh and H. Van Regemorter, J. Phys. B **28**, 3147 (1995).
[5] J. E. Miraglia and J. Macek, Phys. Rev. A **42**, 3971 (1990).
[6] L. I. Men'shikov and P. O. Fedichev, Sov. Phys. JETP **81**, 78 (1995).
[7] M. R. Flannery and D. Vrinceanu, in *Proceedings of the 11th APS Topical Conference,* edited by E. Oks and M. S. Pindzola (AIP Press, New York, 1998), pp. 317–333.
[8] I. Percival and D. Richards, J. Phys. B **12**, 2051 (1979).
[9] R. M. Pengelly and M. J. Seaton, Mon. Not. R. Astron. Soc. **127**, 165 (1964).
[10] Yu. N. Demkov, B. S. Monozon, and V. N. Ostrovskiĭ, Sov. Phys. JETP **30**, 775 (1970).
[11] P. Bellomo, D. Farrelly, and T. Uzer, J. Chem. Phys. **107**, 2499 (1995).
[12] A. Kazansky and V. Ostrovsky, J. Phys. B **29**, 3651 (1996).
[13] A. K. Kazansky and V. N. Ostrovsky, Phys. Rev. Lett. **77**, 3094 (1996); Sov. Phys. JETP **83**, 1095 (1996).
[14] D. Vrinceanu and M. R. Flannery, Phys. Rev. A (to be published).
[15] M. R. Flannery and D. Vrinceanu, Phys. Rev. Lett. **85**, 1 (2000).
[16] M. Gryzinski and J. A. Kunc, J. Phys. B **32**, 5789 (1999).
[17] V. S. Lebedev, J. Phys. B **24**, 1977 (1991).
[18] D. Vrinceanu and M. R. Flannery, Phys. Rev. Lett. **82**, 3412 (1999); Phys. Rev. A **60**, 1053 (1999).
[19] K. G. Kay, Phys. Rev. Lett. **83**, 5190 (1999).
[20] D. Vrinceanu and M. R. Flannery, J. Phys. B **33**, L721 (2000).
[21] M. Born, *The Mechanics of the Atom* (Ungar, New York, 1960), p. 235.